Amplification Schemes and Multi-Channel DBP for Unrepeatered Transmission

L. Galdino, M. Tan, A. Alvarado, D. Lavery, R. Maher, J. D. Ania-Castañón, P. Harper, S. Makovejs, B. C. Thomsen, and P. Bayvel.

***Abstract*— The performance of unrepeatered transmission of a 7 Nyquist-spaced 10 GBd PDM-16QAM superchannel using full signal band coherent detection and multi-channel digital back propagation (MC-DBP) to mitigate nonlinear effects is analysed. For the first time in unrepeatered transmission, the performance of two amplification systems is investigated and directly compared in terms of achievable information rates (AIRs): i) erbium doped fibre amplifier (EDFA) and ii) second order bidirectional Raman pumped amplification. The experiment is performed over different span lengths, demonstrating that, for an AIR of 6.8 bit/s/Hz, the Raman system enables an increase of 93 km (36 %) in span length. Further, at these distances, MC-DBP gives an improvement in AIR of 1 bit/s/Hz (to 7.8 bit/s/Hz) for both amplification schemes. The theoretical AIR gains for Raman and MC-DBP are shown to be preserved when considering low-density parity-check codes. Additionally, MC-DBP algorithms for both amplification schemes are compared in terms of performance and computational complexity. It is shown that to achieve the maximum MC-DBP gain, the Raman system requires approximately four times the computational complexity due to the distributed impact of fibre nonlinearity.**

***Index Terms*— Achievable information rates, coherent detection, forward error correction (FEC), optical fibre communication, Raman amplification, unrepeatered transmission.**

I. Introduction

In submarine systems, the use of repeaters to amplify optical signals significantly increases the system implementation cost due to remote power requirements. Point-to-point unrepeatered links provide a cost-efficient solution for short links, as no in-line active elements are required. These links consist of only passive components, which are essential in connecting islands to the mainland in, e.g., festoon applications.

Increasing both the length and achievable information rate (AIR) in point-to-point unrepeatered links is required to satisfy growing capacity demands. The capacity can be increased by using higher order modulation formats and/or by reducing the frequency spacing between WDM channels. Simultaneously, systems can employ advanced amplification techniques, hybrid fibre spans, or fibre nonlinearity compensation to increase the transmission distance.

Significant progress in unrepeatered transmission has been reported in [1-6]. These experimental investigations were based on transmission of polarization division multiplexed quadrature phase shift keying (PDM-QPSK). In order to increase AIRs, recent efforts have been made towards demonstrating higher order modulation formats in unrepeatered systems [7-12]. However, high order modulation formats require an increased signal-to-noise ratio (SNR), reducing the achievable transmission distance for a given AIR [13-15]. As is well-known, increases in SNR in optical fibre transmission are apparently limited by signal distortions due to fibre nonlinearity; ultimately limiting the achievable transmission distance. However, recent theoretical results have shown that transmission distances can be increased by means of optimal detection in unrepeatered transmission, with no signal-noise interaction [16].

Previously, we demonstrated unrepeatered transmission of PDM 16-*ary* quadrature amplitude modulation (QAM) over single mode fibre (SMF) using multi-channel digital backpropagation (MC-DBP) for fibre nonlinearity mitigation [10, 12]. In the first instance, this was investigated using EDFA receiver pre-amplification (hereafter "EDFA system") [10]. Subsequently, transmission was investigated using 2nd order bidirectional Raman amplification (hereafter "Raman system") [12]. In both cases, the transmission distance was fixed and Q^2-factor (derived from the bit error probability) was used as the system performance figure of merit.

Unlikely previous works, in this paper we are interested in quantifying AIRs as a function of distance from an information theoretic perspective[1]. A (suboptimal) bit-wise decoder where soft bits (logarithmic likelihood ratios) are calculated before being passed to the soft-decision forward error correction (SD-FEC) is considered [14, 19]. An AIR for such systems is the generalised mutual information (GMI), which can be calculated from the received symbols

This work was supported by UK EPSRC Programme Grant UNLOC (UNLocking the capacity of Optical Communications) EP/J017582/1. Lidia Galdino is supported by the National Council for Scientific and Technological Development (CNPQ-Brazil).

L. Galdino, A. Alvarado, D. Lavery, R. Maher, B. C. Thomsen and P. Bayvel are with the Optical Networks Group, University College London, London WC1E 7JE, UK (e-mail: l.galdino@ucl.ac.uk).

M. Tan, I. D. Phillips, P. Harper are with the Aston Institute of Photonic Technologies, Aston University, Birmingham B4 7ET, UK

J. D. Ania-Castañón are with Instituto de Óptica, CSIC, Madrid, 288006, Spain.

S. Makovejs is with Corning Limited, Lakeside Business Village, St. David's Park, Ewloe, CH5 3XD, UK.

[1] The advantages of using AIRs over the prevailing metrics of Q^2-factor or bit error probability for coded optical systems is that it allows a direct estimation of the achievable throughput for a particular transmission system, as highlighted in [17]. Following the work by Secondini et al. [18], in this paper we use the name AIR (instead of e.g., information rate or spectral efficiency) as this name has a precise information-theoretic interpretation.

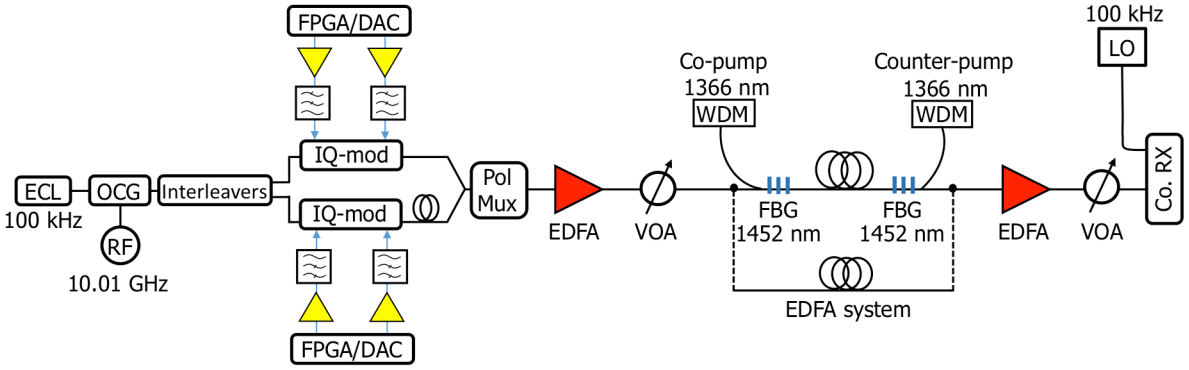

Fig. 1. 7 sub-channel (Nyquist-spaced) PDM-16QAM unrepeatered transmission using EDFA and Raman system.

[Ch. 4, 14], [15]. The performance of capacity-achieving SD-FEC has been shown to follow the GMI prediction. This is the case, e.g., for low-density parity-check (LDPC) codes [Sec. 4, 15], which we consider in this paper.

In this work, we experimentally quantify the AIRs as a function of transmission distance. The system under consideration is unrepeatered transmission of a gross 560 Gb/s (7 x 80 Gb/s PDM-16QAM) Nyquist-spaced superchannel over Corning® SMF-28® ULL fibre. The performance of EDFA and Raman amplification schemes, MC-DBP [13, 20], and the multi-rate LDPC codes were studied. The contribution of this paper is twofold. First, we show experimentally the practical relevance of studying AIR as a function of distance. Second, we use this methodology to investigate different aspects of the unrepeatered transmission system. In particular, we were able to quantify the reach increase offered by the Raman system. Further, we were able to assess the rate penalties associated with practical multi-rate LDPC codes. Finally, the trade-off between the AIR and computational complexity (bandwidth and step size) of MC-DBP was also studied. To the best of our knowledge, this is the first characterisation of the trade-off in MC-DBP complexity in a system incorporating 2nd order bidirectional Raman pump amplification.

This paper is organised as follows. In Sec. II, the experimental setup is described. Sec. III presents the linear and nonlinear DSP and the SD-FEC structure. The transmission performance is analysed in Sec. IV. The MC-DBP computational complexity analysis is presented in Sec. V. Conclusions are drawn in Sec. VI.

II. Experimental Configuration

The experimental configuration is shown in Fig. 1. At the transmitter, an external cavity laser (ECL), at 1550 nm and 100 kHz linewidth, was connected through an optical comb generator (OCG), consisting of a Mach-Zehnder modulator followed by a phase modulator, both overdriven with a 10.01 GHz sinusoidal signal. This configuration generated seven equally-spaced, frequency-locked comb lines. Three cascaded Kylia micro-interferometers were used as interleavers to separate the 7 comb lines into odd and even carriers. Two distinct IQ modulators were used to modulate the odd and even carriers. Four decorrelated pseudo-random binary sequences (PRBS) of length $2^{15}-1$ were digitally generated offline and mapped to 16 QAM symbols, sampled at 2 sample/symbol and shaped using a root-raised-cosine (RRC) filter with 0.1 % roll-off. A linear pre-emphasis was applied to the signal to partially compensate the electrical response of the transmitter. Subsequently, the signals were passed to two digital-to-analogue convertors (DACs) operating at 20 Gsample/s and the DAC outputs were connected to two cascaded 8th order analogue electrical low pass filters, with a cut-off frequency of 7.5 GHz, to remove the images[2]. The odd and even channels were optically decorrelated by 17 ns before being combined and passed through a polarization multiplexing emulation to form the 7 Nyquist-spaced 10 GBd PDM-16QAM channels. The signal power launched into the fibre span, was set using EDFA followed by a variable optical attenuator (VOA), as shown in Fig. 1.

The transmission performance was investigated using two amplification schemes: an EDFA system and a Raman system. In both cases, the optical fibre span was ultra-low loss SMF-28 ULL fibre with an attenuation of $\alpha = 0.165$ dB/km (including splice losses), less than 17 ps/nm/km dispersion and 83 µm² effective area. In the first investigation, the output of the fibre span was connected directly to the EDFA (see Fig. 1) followed by a VOA to adjust the input power to the receiver. Both EDFAs have a noise figure of 5 dB. In the second amplification scheme, highly-depolarised Raman fibre pump lasers at 1366 nm were used as bidirectional pumps. Fibre Bragg gratings (FBGs) centered at 1452 nm with 0.5 nm bandwidth and 95% reflectivity were included at the ends of optical fibre span, thus providing feedback of Stokes shifted 1452 nm light which was used to provide signal amplification in the C-band as shown in [21, 22]. The insertion loss from pump WDM couplers and FBGs was 1.8 dB.

At the receiver side, the signal and LO laser output (100 kHz linewidth ECL) were combined in a super-receiver, comprised by a 90° optical hybrid and balanced photodetectors with 70 GHz electrical bandwidth. A 160 Gsample/s real time sampling oscilloscope with 63 GHz electrical bandwidth was used to sample and digitalise the

[2]The RF signal spectrum from the DAC output, without cascaded analogue electrical low pass filtering and the corresponding output after the filtering with signal pre-emphasis are illustrated in [13].

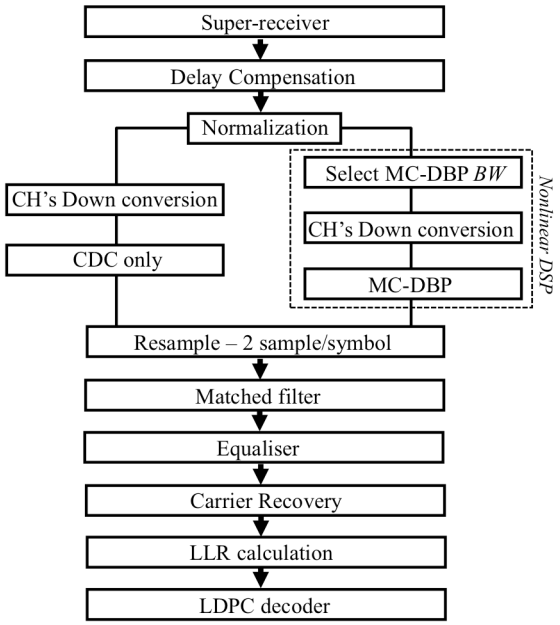

Fig. 2. Digital signal processing chain.

received signals, providing enough bandwidth to coherently receive the full 70 GHz superchannel bandwidth.

III. Digital Signal Processing (DSP)

The digital signal processing (DSP) chain is illustrated in Fig. 2. The DSP of the received signal was performed for compensating the linear impairments in isolation, or applying nonlinear equalization, to mitigate for nonlinear distortion, followed by conventional linear filtering. After DSP was applied, the GMI was estimated from the received symbols and LDPC decoding was performed.

A. Linear DSP

The received signals were initially corrected for receiver skew imbalance and normalised to overcome the response of the balanced photo-detectors in the coherent receiver. Subsequently each channel was down shifted to baseband and chromatic dispersion compensation (CDC) was applied before the signal be resampled at 2 sample/symbol. Frequency domain RRC matched filtering was then applied to each channel. The signal was equalised by applying a 41-tap, using the constant modulus algorithm before switching to a radially directed equalization. The equaliser output was decimated to 1 sample/symbol, whereupon the LO/signal frequency offset was compensated using a fourth power algorithm, followed by decision directed carrier phase estimation for symbol recovery [23].

B. Nonlinear DSP

The nonlinear MC-DBP DSP [13, 20] was applied prior to the linear DSP equalisation. A RRC filter, with zero roll-off, was applied to select the MC-DBP bandwidth (*BW*). The channel of interest was digitally shifted to baseband prior to application of the MC-DBP algorithm, as discussed in [13].

In the EDFA system, the signal power decreases exponentially with distance. Therefore, the exact signal power

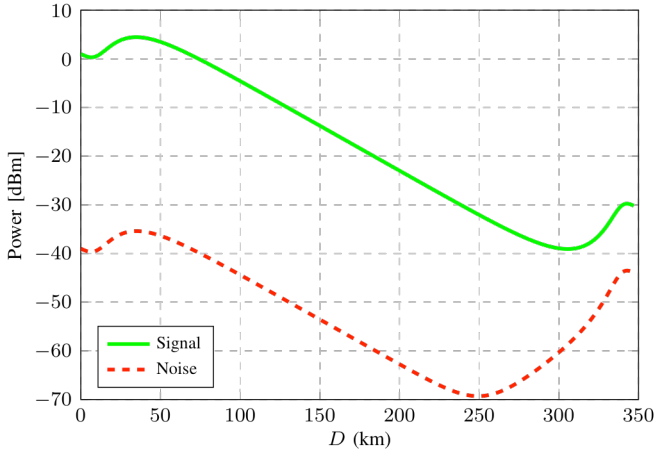

Fig. 3. Simulated signal and noise power distribution over 347 km. Signal launch power of 1 dBm per channel, forward and backward pump power of 30.9 and 31.4 dBm, respectively were considered.

in each MC-DBP step is easily predicted in advance. In the Raman system, the signal power profile requires a more complex calculation to obtain the correct power evolution at each step of the MC-DBP algorithm. In order to obtain the correct power in each step, numerical simulations of the signal power evolution in the Raman system span are required; performed as described in [24]. The experimental parameters, such as Raman gain coefficients, forward pump power, backward pump power, signal launch power, fibre characteristics, need to be included in the model. The simulated signal and noise power distributions over distance $D = 347$ km are shown in Fig. 3.

The MC-DBP algorithm was carried out by solving the Manakov equation using the split-step Fourier method [20]. The optimised number of steps per span was 20 for the EDFA system and 70 for the Raman system. These steps sizes were chosen based on the results illustrated in Fig. 7; further discussion will be presented in Sec. V. A split ratio of 50 % for CDC compensation was used. After MC-DBP, the linear DSP equalisation described previously was applied.

C. SD-FEC

The proposed FEC scheme is a concatenation of an outer hard decision (HD) staircase code (SCC) [25] and an inner irregular repeat-accumulate LDPC code (proposed in the DVB-S2 standard [26]) of rate R_c. In order to obtain a larger family of code rates, the mother LDPC codes were punctured via pseudorandom puncturing patterns. This configuration was previously proposed and used in [19]. The inner LDPC code was implemented offline in Matlab. This enabled the FEC overhead (OH)[3] to be tailored to each of the received PDM-16QAM sub-channels.

The rate of the outer SCC was chosen to be $R_o = 16/17$ (6.25 % *OH*) [27]. This code produces a post-FEC bit error ratio (BER) of 10^{-15} for a post-LDPC BER of $4.7 \cdot 10^{-3}$ [Table I, 27]. If the post-LDPC BER was below the SCC threshold ($4.7 \cdot 10^{-3}$), a post-FEC BER of 10^{-15} was assumed.

[3] In this work, the symbol rate and bandwidth is fixed and the SD-FEC overhead is variable; therefore, the client rate changes according to the applied SD-FEC OH.

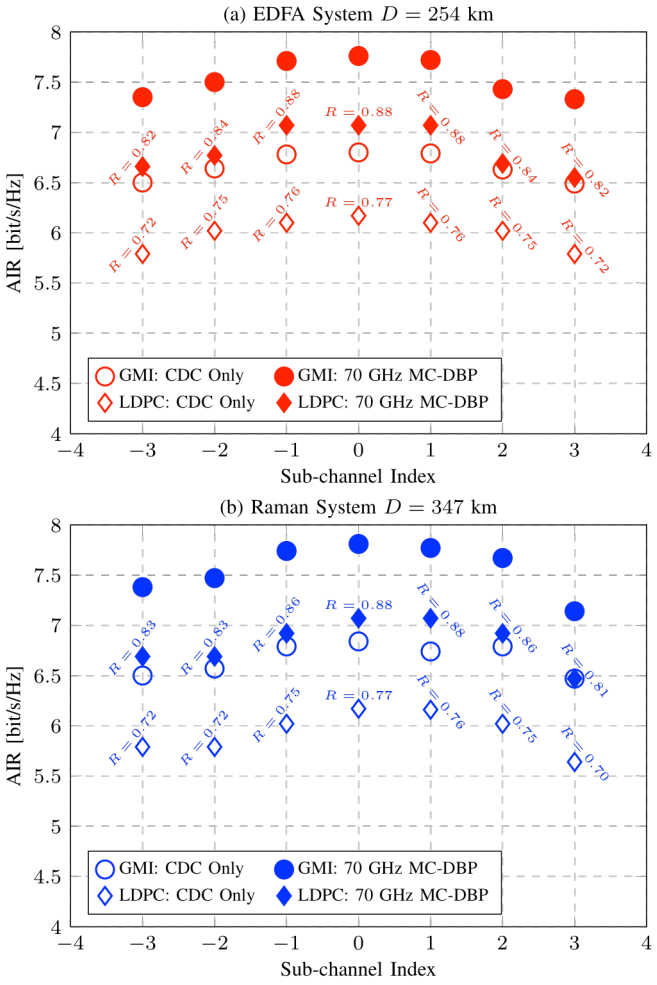

Fig. 4. AIR (at optimum launch power) for each sub-channel with CDC only and 70 GHz MC-DBP bandwidth after transmission over (a) 254 km with EDFA system and (b) 347 km with Raman system.

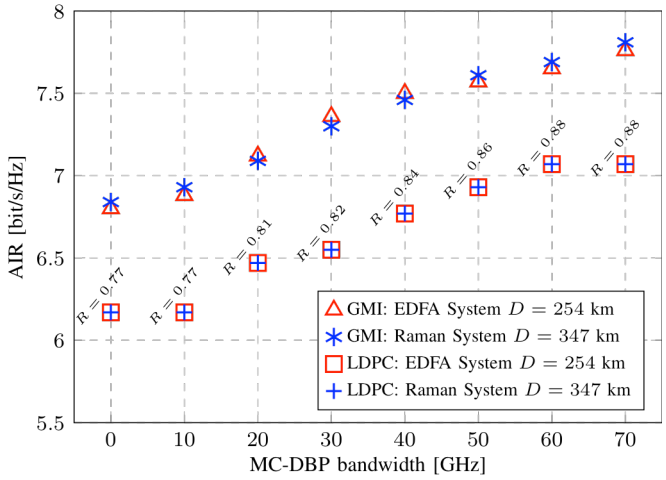

Fig. 5. AIR (at optimum launch power) as a function of MC-DBP bandwidth using EDFA and Raman system.

IV. Unrepeatered Transmission Performance

The unrepeatered transmission system was investigated considering linear and nonlinear impairments compensation. The 7 sub-channels Nyquist-spaced transmitter exhibited a back-to-back (BTB) implementation penalty of 2.2 dB relative to the theoretical SNR limit; at a BER of $4.3 \cdot 10^{-3}$, and required an OSNR of 16.2 dB. The full BTB characterization is described in [13]. The GMI, which is known to predict well the performance of capacity-approaching SD-FEC decoders [14, 15, 19], is used as figure of merit to analyse the system performance.

Fig. 4 illustrates the GMIs (circles) at optimum launch power[4] for all seven sub-channels of the PDM-16QAM signal after transmission over (a) $D = 254$ km using the EDFA system and (b) $D = 347$ km using the Raman system. Empty circles show CDC only results and filled circles show 70 GHz MC-DBP results. Channel '0' represents the central sub-channel of the superchannel. Deterioration in performance towards the edge channels is attributed to the frequency-dependent effective number of bits (ENOB) in the receiver analogue-to-digital converters. For both amplification schemes, the lowest GMI was recorded for the outermost channels. The mean GMI across the channels was 6.66 bit/s/Hz and 6.67 bit/s/Hz for EDFA and Raman systems, respectively. When 70 GHz MC-DBP was applied the mean GMI increased to 7.54 and 7.53 bit/s/Hz, respectively.

The code rates of the inner SD-FEC (R_c) were chosen to match the measured GMIs for each sub-channel following the procedure outlined in [13]. The resulting AIRs for the concatenated coding scheme (LDPC code rate and outer SCC) are shown with diamonds in Fig. 4, and as expected, they follow the GMI prediction. In this figure, the code rates of the coding scheme ($R = R_c \cdot R_o$) for each sub-channel are also shown. The smallest penalty observed with respect to the GMI was 0.66 bit (CDC only and EDFA system), and the largest penalty was 0.74 bit (Raman system with MC-DBP). These penalties are caused by the sub-optimality of the coding scheme under consideration and are in perfect agreement with those reported in [Table III, 19].

As an alternative to a multi-rate approach, the code rate of the LDPC encoder could be chosen based on the minimum GMI across the sub-channels. This has clear implementation advantages as, in this case, only one encoder/decoder pair is required. For MC-DBP (filled diamonds), the minimum code rates in Fig. 4 are 0.82 and 0.81 for the EDFA and Raman systems, respectively. Using these code rates across all the sub-channels results in a penalty of 2.22 % in AIR for both amplification schemes. This small penalty is due to the fact that no large differences in performance are observed across sub-channels, unlike in [13, 28], where the advantage of multi-rate coding is more pronounced.

Fig. 5 illustrates the AIRs for the optimum launch power[5] of the central sub-channel, for different MC-DBP bandwidths after transmission over $D = 254$ km using the EDFA system

[4] For the EDFA system, the optimum launch power was 3 dBm for CDC only and 5 dBm for 70 GHz MC-DBP bandwidth. In the Raman system, the optimum launch power was -7 dBm for CDC only and -4 dBm for 70 GHz MC-DBP bandwidth.

[5] For the EDFA system, the optimum launch power was 3 dBm for 0, 10 GHz MC-DBP, 4 dBm from 20 to 40 GHz MC-DBP and 5 dBm from 50 to 70 GHz MC-DBP. In the Raman system, the optimum launch power was -7 dBm from 0 to 20 GHz MC-DBP, -6 dBm for 30 GHz MC-DBP, -5 dBm for 40 GHz MC-DBP and -4 dBm from 50 to 70 GHz MC-DBP.

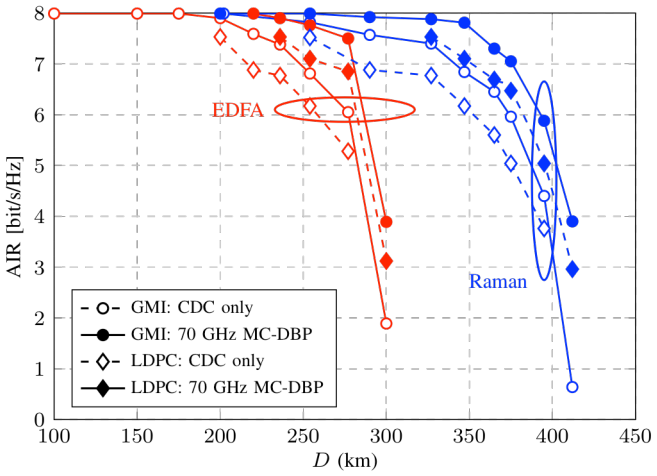

Fig. 6. AIR versus distance (D) using EDFA and Raman system. CDC only and 70 GHz MC-DBP bandwidth performance is also displayed

and $D = 347$ km using Raman system. The GMI results show that MC-DBP provides the same gain in both amplification schemes (approx. 1 bit/s/Hz). Furthermore, for any MC-DBP bandwidth, the GMI of both amplification schemes are almost identical, and thus, the Raman system provides 93 km increase in reach (36 %). Fig. 5 also shows the AIRs obtained by the concatenated coding scheme. For any given MC-DBP bandwidth, the obtained code rate for the EDFA and Raman system were the same. In particular, for CDC only, 29.9 % *OH* was required for reliable transmission, while for 70 GHz MC-DBP the required *OH* was 13.64 %. The obtained increase in AIRs was 0.91 bit (15 %).

Fig. 6 shows the unrepeatered transmission performance ofthe central sub-channel over different distances (D) considering both amplification systems with CDC only and 70 GHz MC-DBP. The code rate (R) of the concatenated coding scheme, the optimum signal launch power per sub-channel, and the forward and backward Raman pump power (optimised as in [21]) used in each amplification scheme (where applicable) are summarised in Table I for the EDFA system and Table II for the Raman system.

As is well-known, and clearly shown in Fig. 6, the use of Raman amplification in a long single fibre span significantly increases performance versus the EDFA system. In particular, these results quantify the gains offered by the Raman system in terms of distance for a given AIR. For instance, for CDC only and an AIR of 7.4 bit/s/Hz, the transmission distance can be increased from $D = 236$ km to up $D = 327$ km by using the Raman system (38 %). Similar gains are observed when comparing the two amplification schemes based on 70 GHz MC-DBP[6]. The results in Fig. 6 also show the dependence of AIR on transmission distance. In particular, there is a sharp degradation in the performance when the distance reaches a

[6] The results shown in Fig. 6 are for the central sub-channel of the superchannel. The gain in performance by applying the Raman system and/or MC-DBP is expected to be the same for the others sub-channels. In the case where the average AIR across all sub-channels is considered, the AIR shown in Fig. 6 is expected to be lower (see Fig. 4), as each sub-channel has a different AIR, but the gain by applying the Raman system is expected to be approximately the same.

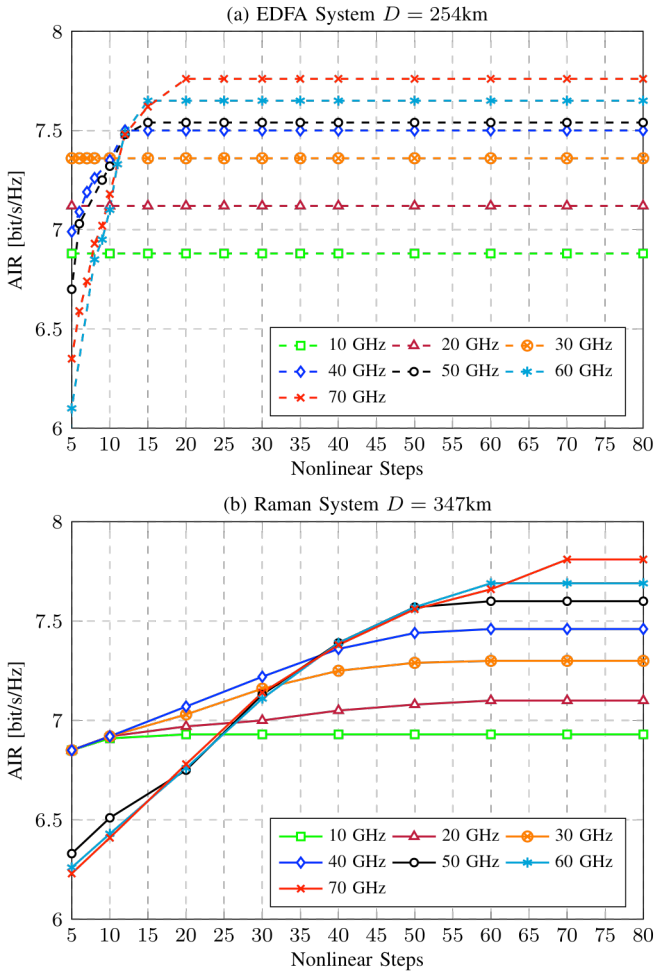

Fig. 7. AIR as a function of the MC-DBP bandwidth and the number of nonlinear steps back propagated for the central sub-channel at a transmission distance over (a) $D = 254$ km using EDFA System and (b) $D = 347$ km using Raman system.

certain value ($D = 277$ km for EDFA system, and $D = 375$ km for Raman system).

When a wide WDM bandwidth is transmitted, a performance degradation of the central sub-channel (when comparing to the 70 GHz bandwidth analysed in this paper) is expected. This is mainly due to additional nonlinear crosstalk. We anticipate that, additionally, the Raman pump power would need to be increased to account for the increased signal bandwidth, and the ASE noise would be increased as a result.

The results in Fig. 6 also show the penalties caused by the concatenated coding scheme under consideration. This also shows that for very short distances, no coding at all was required as the measured pre-LDPC BER was zero ($D \leq 175$ km for EDFA system). There are also two distances ($D = 200$ km for the EDFA system and $D = 254$ km for the Raman system) for which the pre-LDPC BER was already below $4.7 \cdot 10^{-3}$. In these two cases we used the outer SCC only. These results also suggest that QAM constellations with more than 16 constellation points would be a more suitable choice for $D \leq 200$ km. It can also be observed from Fig. 6 that, for distances with high AIRs, MC-DBP does not provide significant gains, as the GMI is already close to the maximum value of 8 bit/symbol. However, when 70 GHz MC-DBP is applied in a system with low AIR, large gains are obtained.

TABLE I

EDFA system: code rate (R) of the concatenated coding scheme as a function of distance (D) for CDC only and 70 GHz MC-DBP, and the optimum signal launch power per sub-channel (S_{power}).

D (km)	R CDC	R MC-DBP	S_{power} (dBm) CDC	S_{power} (dBm) MC-DBP
100	1.00	--	-8	--
150	1.00	--	-7	--
175	1.00	--	-2	--
200	0.94	--	-1	--
220	0.86	--	0	--
236	0.84	0.94	1	4
254	0.77	0.88	3	5
277	0.66	0.85	4	6
300	--	0.39	5	6

For instance, for $D = 412$ km (0.63 bit/s/Hz), MC-DBP provides a gain of 2.87 bits. Similar results were also observed in simulations in [17].

In this paper, second order Raman amplification is investigated (rather than first order) because this scheme reduces the signal power variation along the fibre span, moving the gain towards the middle of the span [22]. Consequently the OSNR is maintained and, thus, an improvement in reach compared with first order Raman amplification is expected. A hybrid Raman/EDFA amplification scheme should give better performance than EDFA because of the ASE noise reduction. However, it would not be as beneficial as bidirectional Raman amplification in unrepeatered systems, as this scheme can simultaneously enhance the signal OSNR and provide Raman gain.

V. MC-DBP Complexity

In the previous section, we showed that MC-DBP provides an increase in the AIR for a specific transmission distance. However, this nonlinear DSP is potentially computationally intensive and sensitive to system parameters compared with the linear DSP. Therefore, this section analyses the required number of nonlinear steps for both the Raman and EDFA systems, and discusses the trade-off in MC-DBP bandwidth and required computational complexity.

Fig. 7 illustrates the AIR estimated from the GMI of the central sub-channel at optimum launch power (same powers as described in footnote 4) for (a) the EDFA system over $D = 254$ km and (b) the Raman system over $D = 347$ km as a function of both the number of nonlinear steps and MC-DBP bandwidth. For the EDFA system, a minimum of 20 steps was required to obtain the highest AIR for 70 GHz MC-DBP bandwidth. As the MC-DBP bandwidth decreased, there was a corresponding decrease in the required number of nonlinear steps per span in order to obtain the highest AIR. However it is evident that for the Raman system at least a minimum of 70 steps were required to obtain the highest AIR for 70 GHz MC-DBP bandwidth, 60 steps for 60 GHz MC-DBP and 50 steps from 20 to 50 GHz MC-DBP bandwidth. The approximately four fold increase in computational complexity for the Raman system is attributed to the large variation in the signal power evolution across the fibre span, particularly on the transmitter side where the signal power was maintained above the launch power for approximately 75 km, as illustrated in Fig. 3. This is in contrast to the EDFA system,

TABLE II

Raman system: code rate (R) of the concatenated coding scheme as a function of distance (D) for CDC only compensation and 70 GHz MC-DBP. The optimum signal launch power per sub-channel (S_{power}), forward Raman pump power (FP_{power}) and backward Raman power (BP_{power}) are also shown.

D (km)	R CDC	R MC-DBP	FP_{power} (dBm)	BP_{power} (dBm)	S_{power} (dBm) CDC	S_{power} (dBm) MC-DBP
200	1.00	--	--		0	3
254	0.94	--	--	31.0	-1	2
290	0.86	--	--	33.0	-2	2
327	0.84	0.94	30.7	31.6	-3	0
347	0.77	0.88	30.9	31.4	-4	1
364	0.70	0.83	31.1	31.4	-6	-3
375	0.63	0.81	31.3	31.4	-7	-4
395	0.47	0.63	31.6	31.6	-8	-5
412	--	0.37	31.8	31.7	-9	-6

where the power profile is monotonically decreasing, following the fibre attenuation profile. It can be concluded that 70 GHz MC-DBP bandwidth should be applied as it gives the highest throughput and the required number of steps is marginally higher for both amplification schemes. Note that this analysis was conducted assuming a uniform step size for the MC-DBP. For both the Raman and EDFA systems the greatest impact of nonlinearity will be incurred close to the transmitter, where the power is relatively high. Therefore, the MC-DBP algorithm could be optimised to take this power profile into account. Note that, if only backward Raman amplification is used, it is expected that the MC-DBP complexity can be significantly reduced compared to bidirectional Raman amplification, as the power close to the transmitter would be the same as the EDFA system.

It has been shown in [13] that chromatic dispersion plays an important role on the MC-DBP performance for repeated long haul transmission systems, especially for a wide backpropagated bandwidth. In unrepeatered transmission systems, the accumulated dispersion is relatively low compared with long haul systems, however, it is still an important parameter to be optimised. For instance, dispersion between 15.9 and 16.2 ps/nm/km was used in the 70 GHz MC-DBP offline signal processing and EDFA system over $D = 254$ km, which gave the highest AIR (7.6 bit/s/Hz). The AIR dropped to 7.3 bit/s/Hz when dispersion of 15.3 or 17.1 ps/nm/km was considered. Similar performance was observed for the Raman system.

VI. Conclusions

This paper experimentally studied the performance of unrepeatered transmission over different distances using full signal band coherent detection and MC-DBP to mitigate for nonlinear distortions. The transmission system performance was investigated using both an EDFA system and a Raman system. Achievable information rates were used as the figure of merit to analyse the transmission performance, and the validity of this approach was verified using LDPC codes. The benefits of the Raman system and MC-DBP were separately estimated. The AIR and complexity of the MC-DBP for each amplification scheme were also analysed.

The Raman system required a smaller step size when

applying the MC-DBP algorithm, thus incurring a computational overhead vs. applying MC-DBP in the EDFA system. However, the MC-DBP complexity analysis was conducted assuming a uniform step size. Therefore, the MC-DBP algorithm could be optimised to take the signal power profile into account, potentially reducing the required complexity in both amplification systems. This analysis is left for future investigations.

This paper considered only PDM-16QAM signals. The results in Fig. 6 suggest that higher order QAM constellations would be a more suitable choice for shorter distances. Transmission considering different modulation formats is left for future work.

ACKNOWLEDGMENT

The authors would like to thank Corning Inc. for supplying the fibre used in this work.

REFERENCES

[1] D. Mongardien, P. Bousselet, O. Bertran-Pardo, P. Tran, and H. Bissessur, "2.6Tb/s (26 x 100Gb/s) unrepeatered transmission over 401km using PDM-QPSK with a coherent receiver," in Proc. ECOC'2009, paper 6.4.3, (2009).

[2] J. D. Downie, J. Hurley, J. Cartledge, S. Ten, S. Bickham, S. Mishra, X. Zhu, and A. Kobyakov, "40 x 112 Gb/s transmission over an unrepeatered 365 km effective area-managed span comprised of ultra-low loss optical fibre," in Proc. ECOC'2010, paper We.7.C.5, (2010).

[3] D. Chang, W. Pelouch, and J. McLaughlin, "8 x 120 Gb/s unrepeatered transmission over 444 km (76.6 dB) using distributed Raman amplification and ROPA without discrete amplification," in Proc. ECOC'2011, paper Tu.3.B.2, (2011).

[4] H. Bissessur, P. Bousselet, D. Mongardien, G. Boissy, and J. Lestrade, "4 x 100Gb/s unrepeatered transmission over 462km using coherent PDM-QPSK format and real-time processing," in Proc. ECOC'2011, paper Tu.3.B.3, (2011).

[5] T. J. Xia, D. L. Peterson, G. A. Wellbrock, P. Doil Chang, P. Perrier, H. Fevrier, S. Ten, C. Towery, and G. Mills, "557-km unrepeatered 100 G transmission with commercial raman DWDM system, enhanced ROPA, and cabled large Aeff ultra-low loss fibre in OSP environment," Proc. OFC/NFOEC'2014, Paper Th5A.7, (2014).

[6] D.Chang, H. Pedro, P. Perrier, H. Fevrier, S. Ten, C. Towery, I. Davis, S. Makovejs, "150 x 120 Gb/s Unrepeatered Transmission over 333.6 km and 389.6 km (with ROPA) G.652 Fibre," in Proc. ECOC'2014, paper Tu.1.5.4 (2014).

[7] D. Mongardien, C. Bastide, B. Lavigne, S. Etienne, and H. Bissessur, "401 km unrepeatered transmission of dual-carrier 400 Gb/s PDM-16QAM mixed with 100 Gb/s channels," in Proc. ECOC'2013, paper Tu.1.D.2, (2013).

[8] J. D. Downie J. Hurley, I. Roudas, D. Pikula, and J. A. Garza-Alanis, "Unrepeatered 256 Gb/s PM-16QAM transmission over up to 304 km with simple system configurations," Opt. Express, Vol. 22, no. 9, pp.10256-61, May (2014).

[9] H. Takara, T. Mizuno, H. Kawakami, Yl Miyamoto, H. Masuda, K. Kitamura, H. Ono, S. Asakawa, Y. Amma, K. Hirakawa, S. Matsuo, K. Tsujikawa, and M. Ymada, "120.7-Tb/s (7 SDM/180 WDM/95.8 Gb/s) MCF-ROPA Unrepeatered Transmission of PDM-32QAM Channels over 204 km," Proc. ECOC'2014, paper PD.3.1 (2014).

[10] L. Galdino, G. Liga, D. Lavery, R. Maher, T. Xu , M. Sato, R. I. Killey, S. J. Savory, B. C. Thomsen and P. Bayvel "Unrepeatered Transmission over 253.4 km Ultra Low Loss Fibre Achieving 6.95 (b/s)/Hz SE using EDFA-only Pre-amplifier," Proc. ECOC'2014, paper P.5.2 (2014).

[11] H. Bissessur, C. Bastide, S. Dubost, S. Etienne, D. Mongardien., "8 Tb/s unrepeatered transmission of real-time processed 200 Gb/s PDM 16-QAM over 363 km," Proc. ECOC'2014, paper Tu.1.5.3 (2014).

[12] L. Galdino, M. Tan, D. Lavery, P. Rosa, R. Maher, I. D. Phillips, J. D. Ania-Castañón, P. Harper, R. I. Killey, B. C. Thomsen, S. Makovejs, and P. Bayvel, "Unrepeatered Nyquist PDM-16QAM Transmission over 364 km using Raman Amplification and Multi-Channel DBP," Optics Letter, Vol.40, no.13, pp. 3025-3028, July (2015).

[13] R. Maher, T. Xu, L. Galdino, M. Sato, A. Alvarado, K. Shi, S. J. Savory, B. C. Thomsen, R. I. Killey and P. Bayvel, "Spectrally Shaped DP-16QAM Super-Channel Transmission with Multi-Channel Digital Back Propagation," Scientific Reports **5**, article number 8214, February (2015).

[14] L. Szczecinski and A. Alvarado, Bit-Interleaved Coded Modulation: Fundamentals, Analysis and Design. John Wiley & Sons, 2015.

[15] A. Alvarado and E. Agrell, "Four-dimensional coded modulation with bit-wise decoders for future optical communications," J. Lightw. Technol. vol. 33, no. 7, pp. 9183–9191, March (2015).

[16] G. Liga, A. Alvarado, E. Agrell, M. Secondini, R. I. Killey, P. Bayvel "Optimum Detection in Presence of Nonlinear Distortions with Memory," in Proc. ECOC'2015, paper P.4.13, (2015)

[17] T. Fehenberger, A. Alvarado, P. Bayvel, and N. Hanik, "On achievable rates for long-haul fibre-optic communications," Opt. Express, Vol. 23 no. 8, pp. 9183-9191, April (2014).

[18] M. Secondini, E. Forestieri, and G. Prati, "Achievable information rate in nonlinear WDM fiber-optic systems with arbitrary modulation formats and dispersion maps," J. Lightw. Technol., vol. 31, no. 23, pp. 3839–3852 (2013).

[19] A. Alvarado, E. Agrell, D. Lavery, R. Maher, and P. Bayvel, "Replacing the Soft FEC Limit Paradigm in the Design of Optical Communication Systems," J. Lightw. Technol., Vol. 33, no. 20, pp. 4338-4352, October (2015).

[20] K. N. Fontaine, et al., "Fiber nonlinearity compensation by digital backpropagation of an entire 1.2-Tb/s superchannel using a full-field spectrally-sliced receiver," in Proc. ECOC'2013, paper Mo.3.D.5, (2013).

[21] P. Rosa, M. Tan, S. T. Le, I.D. Phillips, J. D Ania-Castañón, S. Sygletos, and P. Harper, "Unrepeatered DP-QPSK Transmission Over 352.8 km SMF Using Random DFB Fibre Laser Amplification," Photonics Technology Letters, IEEE, vol. 27, no. 11, pp. 1189-1192, June (2015).

[22] M. Tan, P. Rosa, I. Phillips, and P. Harper, "Extended Reach of 116 Gb/s DP-QPSK Transmission using Random DFB Fibre Laser Based Raman Amplification and Bidirectional Second-order Pumping," Proc. OFC'2015, paper W4E.1, Mach (2015).

[23] I. Fatadin et al., "Blind equalization and carrier phase recovery in a 16-QAM optical coherent system," J. Lightwave Tech. vol. 27 no. 15, pp. 3042-3049, August (2009).

[24] J. D. Ania-Castanon, "Quasi-lossless transmission using second-order Raman amplification and fibre Bragg gratings," Opt. Express Vol. 12 no. 19, pp. 4372-4377, September (2004).

[25] P. B. Smith, A. Hunt, F. R. Kschischang, and J. Lodge, "Staircase codes: FEC for 100Gb/s OTN," J. Lightwave Technol. Vol. 30, no. 1, pp. 110–117, January (2012).

[26] ETSI, "Digital video broadcasting (DVB); Second generation framing structure, channel coding and modulation systems for broadcasting, interactive services, news gathering and other broadband satellite applications (DVB-S2)," ETSI, Tech. Rep. ETSI EN 302 307 V1.2.1 (2009- 08), August (2009).

[27] L. M. Zhang and F. R. Kschischang, "Staircase codes with 6% to 33% overhead," J. Lightw. Technol., vol. 32, no. 10, pp. 1999–2001, May (2014).

[28] A. Ghazisaeidi, L. Schmalen, I. F de Jauregui, P Tran, C. Simonneau, P. Brindel, G. Charlet, "52.9 Tb/s transmission over transoceanic distances using adaptive multi-rate FEC, " in Proc. ECOC'2014, Postdealine paper, (2009).